Absolute Electron Impact Ionization Cross Section for N20 and NO from Threshold up to 1000 eV.

I. Iga[#], M. V. V. S. Rae* and S. K. Srivastava

Jet Propulsion Laboratory
California Institute of Technology
4800 Oak Grove Drive, Pasadena, California 91109

[#]Visiting fellow, on leave of absence from Universidade Federal de Sao Carlos, Departamento de Quimica, 13560, Sao Carlos, SP, Brazil

*NRC NASA Resident Research Associate, on leave of absence from Institute for Plasma Research, Bhat, Ghandinagar - 382424, India

ABSTRACT

Normalized values of cross sections for the production of ions by electron impact on N20 and NO have been obtained by utilizing the relative flow technique. The accurately known values of cross sections for the production of singly charged ions of rare gases from the parent atoms have been used for the normalization. Cross sections for the generation of fragment ions have been measured for the first time. By summing the cross sections for the direct ionization and dissociative ionization, total ionization cross sections have been obtained and compared with the previously available data. Energies for the appearance of various ions have also been measured and compared with predictions of the photoelectron spectroscopy and Hess's law.

1. INTRODUCTION

Nitric and nitrous oxide are important molecules for the chemistry of the ionosphere. NO^+ is one of the most abundant species in the thermosphere and also one of the major reactant at lower altitudes. In the lower E- and D- region it undergoes reactions[1,2] with other atmospheric gases and plays an important role in the clustering of proton hydrates. Since NO^+ can result from the ionization and dissociative ionization of NO and N_2O, many studies[3-11] have been directed towards photon and electron impact ionization and fragmentation properties of these molecules. However, to date there have been very few measurements on the electron impact ionization and dissociative ionization cross sections of them which are important for modeling the earth's ionosphere. For example, no cross section values have been reported for dissociative ionization of nitrous and nitric oxide so far. Only the values of absolute cross sections for direct ionization have been published[12,13] in the literature for both molecules and the maximum electron impact energy range has been restricted to 180 eV. Total ionization cross sections and total cross sections for the formation of fragment ions with kinetic energies larger than 0.25 eV have also been measured[14,15] for both molecules in the energy range of threshold to 1000 eV.

The paucity of cross section data regarding dissociative ionization processes can be attributed to technical difficulties related to complete collection of energetic fragment ions from the ionization region. However, recent developments such as the fast beam technique[16] and the pulsed ion extraction technique[17] have provided satisfactory results in the past and reliable values of dissociative ionization cross sections are now available for a few molecules.

As a part of a continuing program in our laboratory for the measurement of ionization cross sections of various atomic and molecular species we have obtained cross sections for the formation of N+, O^+ and NO^+ from nitric oxide and N+, O^+, N_2^+, NO^+ and $N2O^+$ from nitrous oxide. Total ionization cross sections have also been derived by the summation of all partial and dissociative ionization cross sections.

2. EXPERIMENTAL PROCEDURE AND APPARATUS

The experimental procedure, apparatus, and error estimation have been described in detail in our previous publications (ref. 17 and references cited therein) . Basically the apparatus, schematically shown in figure 1, has the crossed electron beam- molecular beam collision geometry. The molecular beam is produced by flowing the gas of interest through a capillary array which keeps it confined[18] in a beam of diameter close to 1mm. The electron beam which intercepts the molecular beam at 90° is produced by thermionic emission from a heated tungsten hairpin filament, followed by magnetic collimation by an axial field of about 100 G or less by a solenoid. The electron beam has a diameter close to 0.5 mm. Therefore, the scattering volume is estimated to be less than $1mm^3$.

As a result of collisions ions are produced. They are extracted out of the collision region by a pulsed extraction technique. An important property of this technique is that very high extraction fields can be applied close to the interaction region without disturbing the electron beam. Details on the pulsed extraction technique can be found in the publication by Krishnakumar and Srivastava[19].

For the experimental determination of the variation of the

ionization efficiency of a molecule dissociating into a particular ionic species as a function of the electron impact energy the ion of interest is mass selected by the quadruple or time of flight mass spectrometer and its intensity is stored in a multichannel analyzer. The resulting spectra for various ionic species are called "ionization efficiency curves". Since the extraction efficiency, transmission efficiency, and charge particle detection efficiency of the detector do not depend on the electron impact energy no corrections to the shapes of these curves are normally required. However, the "overlap volume", defined by the overlap of the electron beam, molecular beam, and view cone of the detector, changes with the electron beam energy. Therefore, the gas under investigation and helium (He) gas are flowed together and the ionization efficiency curves for both are recorded one after the other. Since the shape of helium ionization efficiency curve is well known[19] the variation of the overlap volume can be corrected. The measured ionization efficiency curve for the ion of interest is normalized to obtain absolute values of cross sections. They are obtained by the application of the relative flow technique[20-22]. Briefly, this technique utilizes ionization cross sections for rare gases[19] as standards to calibrate the ionization spectrometer. The calibration factors thus obtained are then utilized to derive the absolute values of cross sections.

The error estimation follows the procedure described by Krishnakumar and Srivastava[22]. Typically an error of ±3% is estimated in the shape of the ionization efficiency curve. The cross section values are estimated to be uncertain by ±15%.

The onsets for different channels of production of ions are determined by the points of intersections generated by lines drawn through the various slopes in the ionization

efficiency curve. For example, in figure 2 four lines have been drawn for four different slopes which are clearly discernible in the shape of ionization efficiency curve for the production of N^+ from N20. The first line intercepts the X axis at 20 eV. The others cross each other at 26.2, 31.4 and 35.3 eV. The electron impact energy is calibrated by measuring the thresholds for He^+ and Ar^+ resulting from the ionization of He and Ar, respectively. It is estimated that the energy spread is about 0.5eV.

3. RESULTS AND DISCUSSION

Collisions of energetic electrons with N20 and NO can give rise to a large number of processes which can result in the formation of ions. Among them the following ones have been studied by us:

$$e^- + N20 \rightarrow N_2O^+ + 2e^-, \quad (1)$$
$$\rightarrow NO^+ + \text{other fragments}, \quad (2)$$
$$\rightarrow N_2^+ + \text{other fragments}, \quad (3)$$
$$\rightarrow N^+ + \text{other fragments}, \quad (4)$$
$$\rightarrow O^+ + \text{other fragments}, \quad (5)$$

$$e^- + NO \rightarrow NO^+ + 2e^-, \quad (6)$$
$$\rightarrow N^+ + \text{other fragments}, \quad (7)$$
$$\rightarrow O^+ + \text{other fragments}, \quad (8)$$

where other fragments may consist of both ionized and neutral species. Cross sections for processes(1) and (6) are generally called partial or direct ionization cross sections and we will represent them by symbol σ_p. Cross sections for other processes are named dissociative ionization cross section and we will indicate them by the symbol σ_d. The total ionization cross section, σ_T, is a sum of all the above processes plus other ones which may result in the formation of ions such as multiply charged ions and ions

resulting from the inner shell excitations. However, the magnitudes of all other processes are generally much lower than the ones mentioned above. Therefore, the values of σ_T obtained from the summation of σ_p and σ_d are very close to the actual values (in our estimate the present results should be within 5% of the actual values) . The sum of all dissociative ionization cross section gives the total dissociative ionization cross sections represented by the symbol $\sigma_d{}^T$.

We have measured the values of σ_p and σ_d for both molecules and summed them up to obtain the values of σ_T. Tables I and II present our values of cross sections for N20 and NO, respectively. They are also shown in figures 3 and 4 along with previously published data.

In Figure(3) , curve(1) represents our values of total ionization cross sections for nitrous oxide, where the values reported by Rapp and Englander- Golden[14] are also shown. The agreement between the two results is excellent over the entire electron impact energy range.

The ionization efficiency curve for formation of N_2O^+ is shown in Fig.(3) as curve(2). For this ion its production starts at about 12.3 eV, reaches a maximum around 100 eV and smoothly decreases as the energy increases to 1000 eV. The solid diamonds represent measurements of Mark et al. 13 from threshold to 180 eV. Although their ionization efficiency curve has similar shape as ours the magnitudes of their cross sections are about 30% lower than the present measurements at 100 eV. Our ionization efficiency curve lifts off from the X axis at 12.3 eV and changes its slope at about 14.2 eV indicating that some new channel for the production of $N20^+$ begins at this energy.

The threshold for N_2O^+ production, given by photoelectron

spectroscopy, is 12.89 eV (Ref. 23). The agreement between our value and this result is excellent considering the fact that our measurements are uncertain by about 0.5 eV. The ionization channels producing excited states of N_2O^+ occur at 16.39 eV, 18.23 and at 20.105 eV, respectively, for the states A $^2\Sigma^+$, B $^2\pi$ and C $^2\Sigma^+$. Therefore, the change of slope for N_2O^+ production at 14.2 eV must be associated with some other process. Photoionization mass spectrometry studies[24] have reported that the neutral Rydberg states converging to the A $^2\Sigma^+$ ionic state interact with two continua $(X^2\pi)+e^-$ and $(^4A'')+e^-$. $(X^2\pi)$ continuum leads only to N_2O^+ production whereas $(^4A'')$ leads to N_2O^+ and O+.

Cross sections for the production of NO^+ are presented in figure(3) by curve(3). In the present studies the onset for the production of NO^+ from N20 is observed at about 16.2 eV Furthermore, additional changes in the slope of the ionization efficiency curve are seen at 19.5 eV and 21.5 eV. The rate of production of NO^+ increases by about 2.8 and 1.4 times, respectively, at the two slopes. Thermochemical calculations[25] show that the onset for the process leading to NO^+ + N from N20 should be 14.19 eV. However, our results indicate this to be at 16.2 eV which is higher. Thus, 2 eV must be shared by NO^+ and N in the form of kinetic energies of these fragments.

For N_2^+ (Fig. (3)-curve(4)) the onset begins at 17.5 eV. Two changes in the slope occur at 21.3 and 24.1 eV. The production of N_2^+ increases by about a factor of 3.5 and 1.6 at these slopes. Thermochemical calculations[25] predict the threshold energy for the process leading to N_2^++O to be 17.25 eV which is in excellent agreement with the present measurements.

For N^+ (Fig. (3)-curve(5)) the onset begins at 20 eV and it is followed by 3 changes in the slope of the ionization

efficiency curve at 26.2, 31.4 and 35.3 eV with increments in the rate of production of N^+ by factors of 2.8, 1.5 and 1.3, respectively. Thermochemical calculations[25] show that the production of N+, through the process $N^+ + NO$, should begin at 19.47 eV which is in good agreement with the present results.

Our measurement show that 0^+ (Fig.(3)- curve(6)) appears at the electron impact energy of 16.01 eV followed by a change of slope at 18.5 eV. Thermochemical calculations[25] predict a value of 15.29 eV for the onset for the reaction leading to the production of $O^+ + N_2$ from N_20. However, our value is higher by about 0.72 eV which indicates that the two fragments, 0^+ and N2, share this excess energy in the form of kinetic energy.

The total dissociative ionization cross section, σ_d^T, is also shown in figure(3) by curve(7). This curve was obtained by adding the cross sections for the production of all fragment ions from N20. Our results are compared with the measurements of Rapp et al 15 which are for ions with kinetic energies larger than 0.25 eV. Both of them agree well with each other in shape as well as in magnitude.

Figure (4) shows ionization efficiency curves for ions resulting from NO. Curve (1) represents total ionization cross sections, σ_T. Our results are higher by about 18% than the values reported by Rapp and Englander- Golden[14]. However within the error limits of the two experiments the agreement is satisfactory.

Our measurements indicate that the threshold for the production of NO^+ is about 9.6 eV (Fig.4-curve(2)) which is in excellent agreement with the value of 9.26 eV reported by photoelectron studies[23]. The ionization efficiency curve rises steeply peaking up at about 100 eV and then slowly

decreases towards higher electron impact energies. The measurements of Kim et al.[12], on the other hand, show (Fig. 4) a maximum at about 80 eV electron impact energy and rapid decrease in cross sections at higher energies. Their cross sections are lower by about 19% at 100 eV than the present ones.

Figure 4 curve(3) shows the ionization efficiency curve for the production of N^+ ions from NO. The onset for their production is about 24.6 eV. It rises smoothly and reaches a maximum at about 100 eV. Although it is not obvious from this figure our detailed investigation near the threshold region shows a change in the slope of the curve near 28.1 and 34.0 eV. Similar is the situation with the production of 0^+ from NO which has an onset at about 20.4 eV and a change of slope near 25.3 eV.

Figure(4) curve(5) presents total dissociative ionization cross sections, σ_d^T, where the present results are compared with the previous data of Rapp et al.[15] who measured cross sections for the productions of all fragment ions with kinetic energies larger than 0.25 eV. Our results are smaller by about 17% than their's at 100 eV. Considering the error limits of the two experiments the agreement is satisfactory.

4. CONCLUSIONS

We have measured cross sections for the production of ions by electron impact on N20 and NO and compared them with previous results. The data for dissociative ionization are presented for the first time and are valuable for modeling the various plasmas. Our measured threshold energies for the production of various ions are, in general, in good agreement with the results obtained by the photoelectron spectroscopy. Our studies show that NO^+ and N fragments from

the dissociation of N20 are produced with appreciable amount of kinetic energies which may have important effect on the chemistry of the ionosphere.

ACKNOWLEDGEMENTS

The research described in this paper was performed at The Jet Propulsion Laboratory/ California Institute of Technology, under contract with the U.S. Airforce Office of Scientific Research and the National Aeronautics and Space administration. Iga gratefully acknowledges support from FAPESP(Fundacao de Amparo a Pesquisa do Estado de Sao Paulo) , CNPq(Conselho National de Desenvolvimento Cientifico e Tecnologico) and Finep(Financiadora de Pesquisas e Projetos) . Rao thanks NRC/NASA for a resident research associateship grant.

5. REFERENCES

1. D. Krankowsky, P. Lammerzahl, A. Götzelmann, M. Friedrich and K. M. Torkar, J. atmos. terr. Phys. 49, 809 (1987).

2. " Potential Energy Surfaces for Air Triatomics", Vol. I- Literature Review, National Bureau of Standards prepared for Aerospace Research Laboratories, National Research Council, Argonne National Laboratory, June 1975.

3. J. H. D. Eland, Int. J. Mass Spectr. Ion Phys 12, 389 (1973) .

4. B. Brehm, R. Frey, A. Kustler, J. H. D. Eland, Int. J. Mass Spectr. Ion Phys. 13, 251 (1974).

5. I. Nenner, P. M. Guyon, T. Baer and T. R. Govers, J. Chem. Phys. 72, 658 (1980).

6. J. L. Olivier, R. Locht and J. Momigny, Chem. Phys. 68, 201 (1982).

7. T. Ibuki and N. Sugita, J. Chem. Phys. 80, 4625 (1984).

8. J. L. Olivier, R. Locht and J. Momigny, Chem. Phys. 84, 295 (1884).

9. M. Hamdan, F. M. Harris, I. W. Griffiths and J. H. Beynon, Chem. Phys. Lett. 135, 511 (1987).

10. R. Locht, G. Hagenow, K. Hottmann and H. Baumgartel, Chem. Phys. 151, 137 (1991).

11. M. Takahashi, H. Ozeki and K. Kimura, Chem. Phys. Lett. 181, 255 (1991).

12. E. Mark, T. D. Mark, Y. B. Kim and K. Stephan, J. Chem. Phys. 75, 4446 (1981).

13. Y. B. Kim, K. Stephan, E. Mark and T. D. Mark, J. Chem. Phys. 74, 6771 (1981).

14. D. Rapp and P. Englander- Golden, J. Chem. Phys. 43, 1464 (1965).

15. D. Rapp, P. Englander- Golden and D. D. Briglia, J. Chem. Phys. 42, 4081 (1965).

16. F. A. Baiocchi, R. C. Wetzel and R. S. Freund, Phys. Rev. Lett. 53, 771 (1984).

17. E. Krishnakumar and S. K. Srivastava, J. Phys. B: At. Mol. Opt. Phys. 23, 1893 (1990).

18. R. T. Brinkmann and S. Trajmar, J. Phys. E: Sci. Instrum. 14, 245 (1981).

19. E. Krishnakumar and S. K. Srivastava, J. Phys. B: At. Mol. opt . Phys. 21, 1055 (1988).

20. S. K. Srivastava, A. Chutjian and S. Trajmar, J. Chem. Phys. 63, 2659 (1975).

21. 0. J. Orient and S. K. Srivastava, J. Phys. B: At. Mol. Phys. 20, 3923 (1987).

22. E. Krishnakumar and S. K. Srivastava, Phys. Rev. A41, 2445 (1987).

23. D. W. Turner, A. D. Baker, C. Baker and C. R. Brundle, "Molecular Photoelectron Spectroscopy", Wiley, London

(1970) .

24. J. Berkowitz and J. H. D. Eland, J. Chem. Phys. 67, 2740 (1977) .

25. J. Berkowitz, " Photoabsorption, Photoionization and Photoelectron Spectroscopy", Academic Press, New York, San Francisco, London (1970).

Table 1.

Partial and total ionization cross sections of N20 by electron impact (in units of 10^{-18} cm^2)

Energy (eV)	N_2O^+	NO^+	N_2^+	N^+	O^+	σ_T	σ_d^T
20	41.4	5.45	0.67		0.67	47.57	6.19
30	100.0	30.9	1.60	3.20	5.60	151.3	51.3
40	147.0	52.7	20.0	8.60	9.00	237.3	90.3
50	171.2	68.2	25.4	15.9	13.9	294.6	123.4
60	182.2	77.3	28.6	20.4	14.9	323.4	141.2
70	187.7	81.8	30.2	24.7	15.8	340.2	152.5
80	191.8	83.6	30.4	28.9	16.1	350.8	159.0
90	194.5	84.5	30.4	31.2	16.2	356.8	162.3
100	195.9	85.4	30.9	32.4	16.5	361.1	165.2
110	195.3	86.4	31.4	33.3	16.5	362.9	167.6
120	194.5	86.4	31.4	33.8	16.5	362.6	168.1
130	193.0	86.8	31.4	34.1	16.4	361.7	168.7
140	191.0	86.4	30.9	34.2	16.3	360.5	167.8
150	189.2	85.9	30.9	34.2	16.1	356.3	167.1
160	187.7	85.4	30.7	34.1	15.9	353.8	166.1
170	185.8	84.5	30.2	33.6	15.6	349.7	163.9
180	183.0	84.1	29.5	33.3	15.6	345.5	162.5
190	180.8	83.6	29.1	32.8	15.2	341.5	160.7
200	178.1	82.3	28.2	31.9	15.0	335.5	157.4
225	171.7	80.5	26.8	30.2	14.1	323.2	151.6
250	166.2	76.8	25.6	28.2	13.4	310.2	144.0
275	159.8	73.2	24.5	26.3	12.6	296.4	136.6
300	153.4	70.9	23.3	24.6	11.9	284.4	130.7
350	141.6	64.5	21.2	21.1	10.8	259.2	117.6
400	132.5	59.5	19.3	18.8	9.70	239.8	107.3
500	113.1	51.8	16.7	15.1	8.30	205.0	91.9
600	102.5	46.4	14.9	12.9	7.20	183.9	81.4
700	91.9	41.8	13.7	11.1	6.70	165.2	73.3
800	84.8	40.0	13.0	10.2	6.20	154.2	69.4
900	81.3	38.9	12.3	9.50	6.00	148.0	66.7
1000	77.7	38.2	11.9	9.00	5.70	142.5	64.8

Table 2.

Partial and total ionization cross sections of NO by electron impact (in units of 10^{-18} cm^2)

Energy (eV)	NO^+	N^+	O^+	σ_T	σ_{d^T}
10	1.06			1.06	
20	40.0			40.0	
30	120.0	4.38	2.74	127.1	7.12
40	264.1	15.3	7.67	243.0	23.0
50	280.9	26.9	11.0	301.9	37.8
60	287.5	34.5	13.7	329.2	48.2
70	287.4	40.8	16.4	343.8	57.3
80	289.7	44.4	17.5	349.4	61.9
90	289.7	47.1	18.4	355.2	65.5
100	290.2	47.9	18.9	357.1	66.8
110	289.3	48.1	18.9	356.3	67.0
120	287.4	48.2	19.5	355.1	67.7
130	286.5	47.7	19.8	354.0	67.5
140	283.7	47.1	19.7	350.6	66.9
150	280.9	46.6	19.7	347.3	66.3
160	278.1	46.3	19.2	343.6	65.5
170	275.0	46.1	19.2	340.2	65.2
180	272.6	45.5	18.6	336.7	64.1
190	267.9	45.0	18.5	331.4	63.5
200	264.1	44.5	18.3	326.9	62.8
225	254.1	42.6	17.7	313.9	59.9
250	244.6	40.7	17.0	302.2	57.7
275	233.6	38.9	16.4	288.9	55.2
300	225.4	37.0	15.7	278.1	52.7
350	206.4	32.8	13.4	253.1	46.7
400	188.6	29.3	10.5	230.2	41.5
500	162.7	24.1	12.2	197.3	34.5
600	143.6	20.9	10.5	174.0	30.3
700	132.7	18.1	9.42	159.6	26.9
800	120.4	16.7	8.37	145.6	25.1
900	116.3	14.7	7.67	134.6	22.3
1000	106.8	13.2	7.67	127.7	20.9

FIGURE CAPTIONS

Figure 1. Schematic of the experimental arrangement.

Figure 2. Ionization Efficiency Curve for the production of N^+ from nitrous oxide near the threshold. Figure illustrates the various onsets and method for obtaining their values.

Figure 3. Ionization Efficiency Curves for various ions from nitrous oxide from threshold to 1000 eV. Curve(l): present values for Total Ionization Cross Section, σ_T. Sol id circles: σ_T values given by Rapp and Englander- Golden; Curve(2) : present values for Direct or Partial Ionization Cross Section, up. Solid diamonds: measurements of σ_p by Mark et al.; Curves (3)-(6) : present values of Dissociative Ionization Cross Section, σ_d, for the fragments NO+, N_2^+, N^+ and 0^+; Curve(7): present values of Total Dissociative Ionization Cross Section, σ_d^T. Filled triangles: Dissociative Ionization Cross Section values for ions with kinetic energies > 0.25 eV measured by Rapp et al.

Figure 4. Ionization Efficiency Curves for various ions from nitric oxide from threshold to 1000 eV. Curve(l): Present values of Total Ionization Cross Section, σ_T. Open diamonds σ_T values given by Rapp and Englander- Golden. Curve(2): present values for partial ionization cross section, σ_p. Solid diamonds: up values given by Stephan et al. curves(3) and (4): dissociative ionization, σ_d for N^+ and 0^+. curve(5) : total dissociative ionization cross section, σ_d^T, filled triangles: dissociative ionization cross section values for ions with kinetic energies >.25 eV measured by Rapp et al.

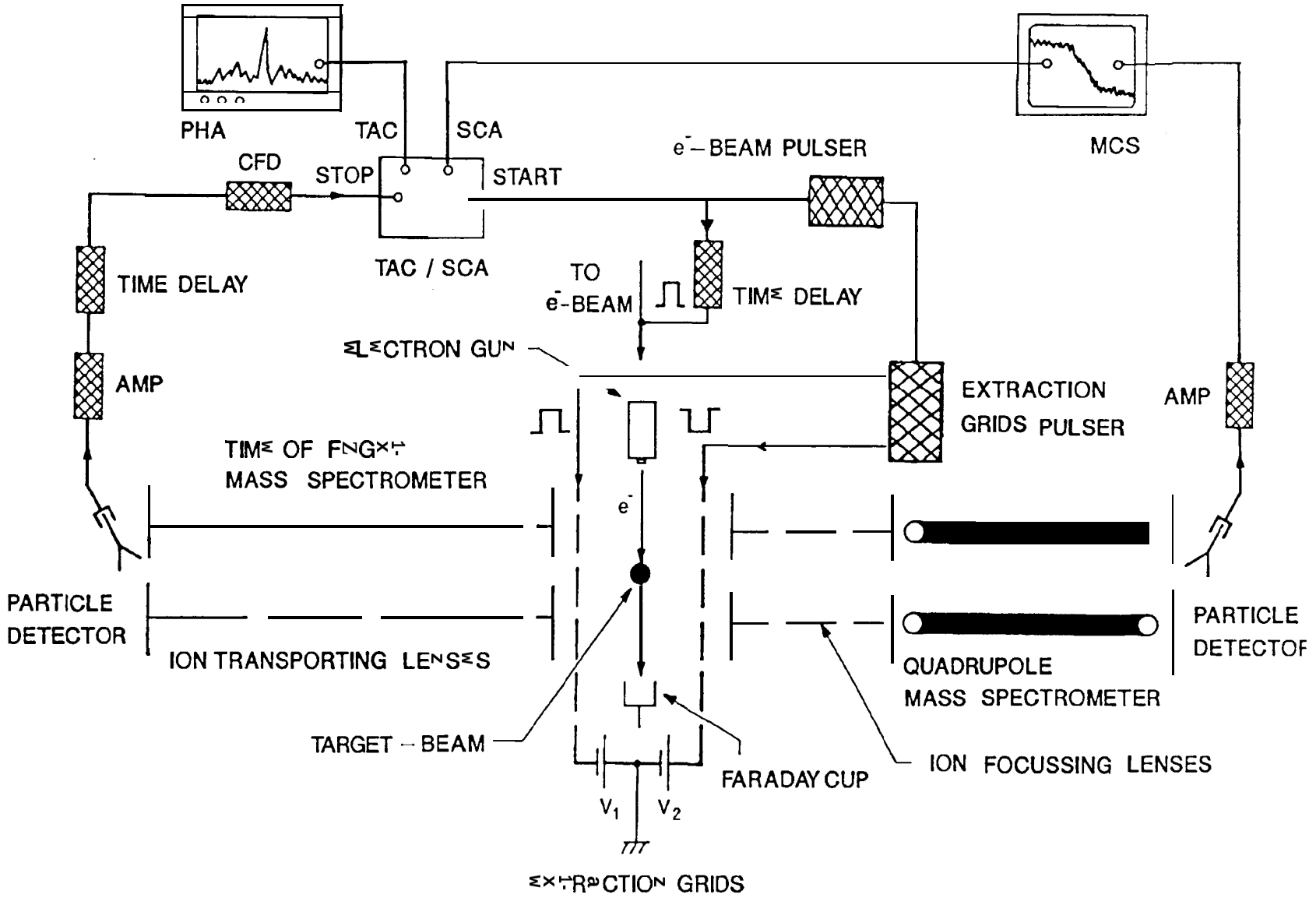
PHA
TAC
SCA
MCS
CFD
STOP
START
e⁻ – BEAM PULSER
TAC / SCA
TIME DELAY
TO
e⁻-BEAM
TIME DELAY
ELECTRON GUN
AMP
EXTRACTION
GRIDS PULSER
AMP
TIME OF FLIGHT
MASS SPECTROMETER
e⁻
PARTICLE
DETECTOR
ION TRANSPORTING LENSES
PARTICLE
DETECTOR
QUADRUPOLE
MASS SPECTROMETER
TARGET – BEAM
FARADAY CUP
ION FOCUSSING LENSES
V1
V2
EXTRACTION GRIDS

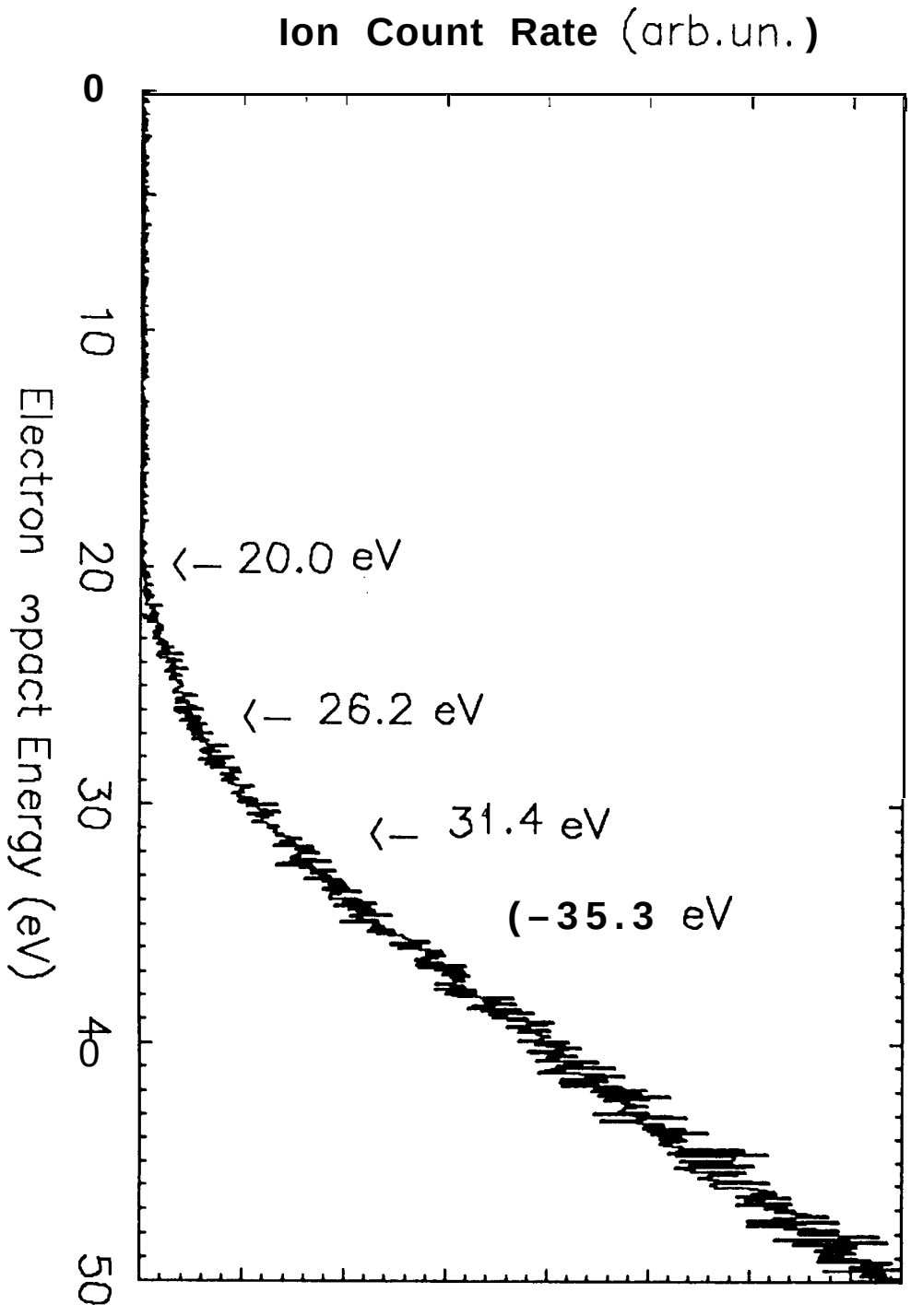
Ion Count Rate (arb.un.)
0
10
20
30
40
50
Electron Impact Energy (eV)
<– 20.0 eV
<– 26.2 eV
<– 31.4 eV
(–35.3 eV

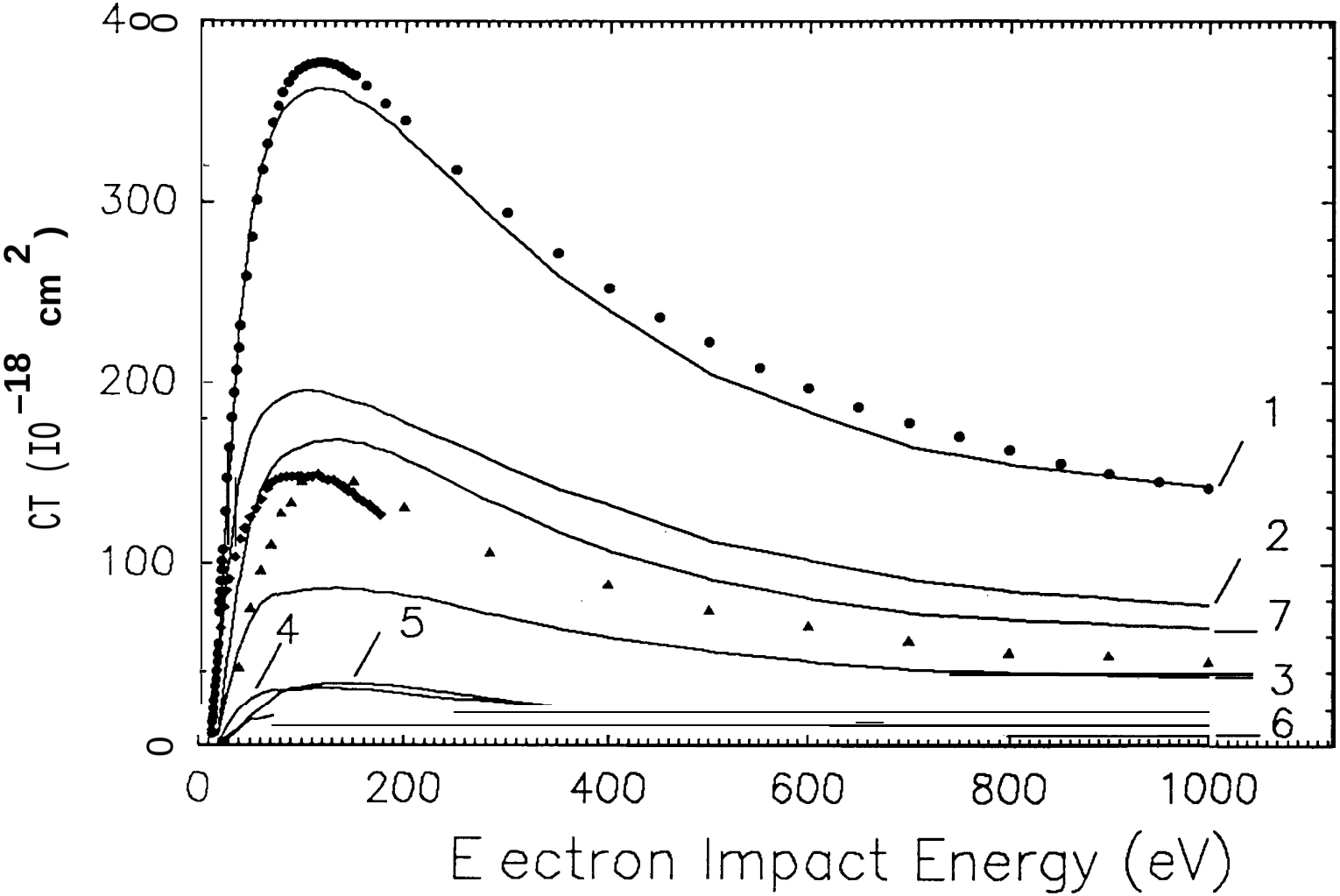
400
300
200
100
0
CT (I0^{-18} cm^2)
0
200
400
600
800
1000
E ectron Impact Energy (eV)
1
2
7
3
6
4
5

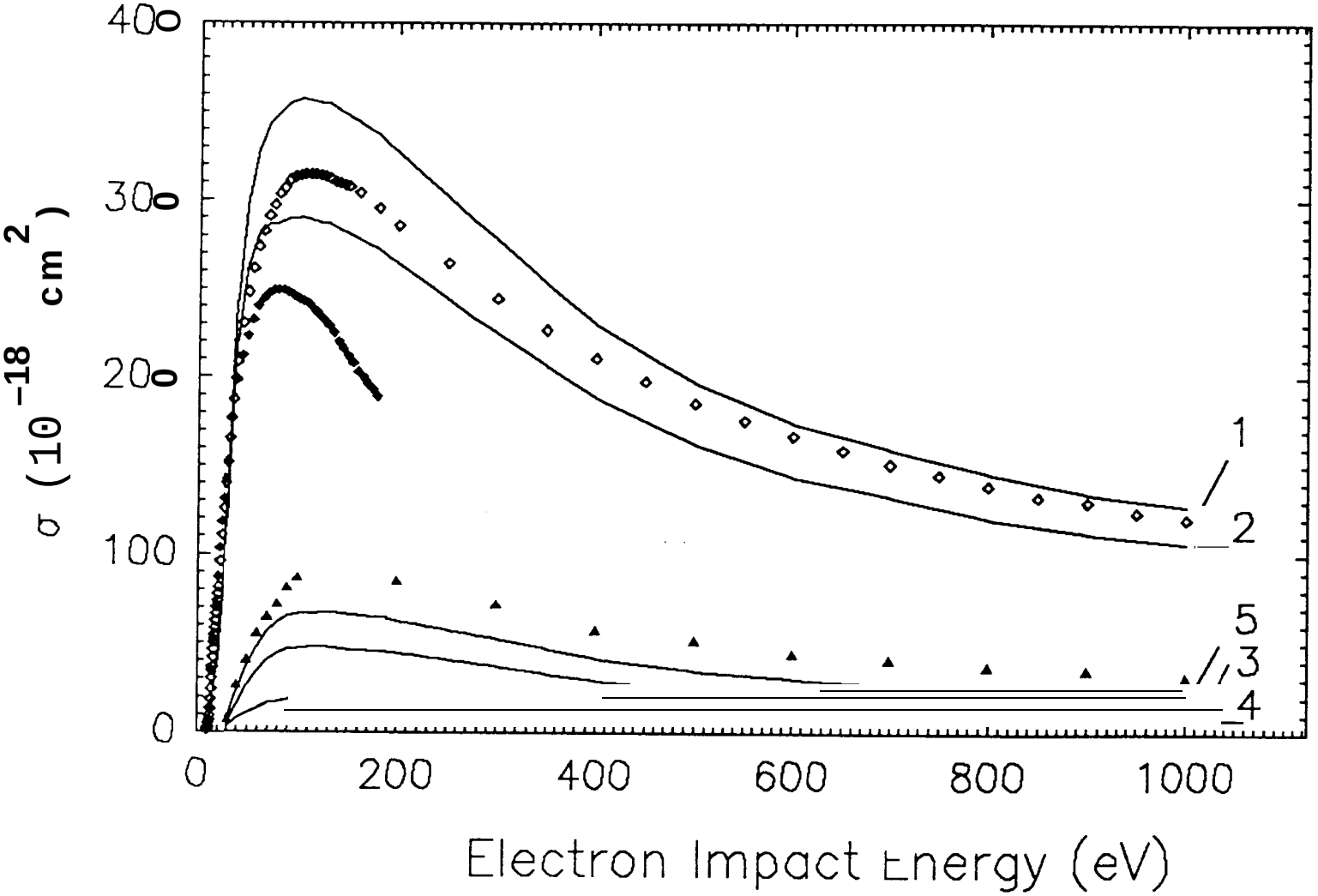
400
300
200
100
0
σ (10^-18 cm^2)
0
200
400
600
800
1000
Electron Impact Energy (eV)
1
2
5
3
4